Macalester Journal of Physics and Astronomy

Volume 1
Issue 1 *Spring 2013*

Article 15

1-28-2014

Photometric and Spectroscopic Analysis of Young, Nearby Open Cluster Collinder 70

Clara M. Thomann
Macalester College, claramthomann@gmail.com

Photometric and Spectroscopic Analysis of Young, Nearby Open Cluster Collinder 70

Clara M. Thomann[1], David D. James[2], Owen Boberg[3], Phillip Cargile[4], and Alicia Aarnio[5]

Cerro Tololo Inter-American Observatory, La Serena, Chile

ABSTRACT

We present the results of a wide-field (80' x 80') photometric and spectroscopic survey of the young open cluster Collinder 70, which is also known as the ORI OB 1b association, centered on the central star of Orion's belt, ϵ Ori (Alnilam). Seventy Coll 70 spectroscopy targets were selected from BVRIc color magnitude diagrams for observation using the CTIO HYDRA multi-object spectrograph; we aimed to identify targets exhibiting Hα in emission and a strong lithium 6708Å line in absorption. About a third of our targets (23/70 stars) are consistent with being youthful members of Coll 70. Intermediate resolution (R$\sim$20000) HYDRA Li I 6708Å equivalent widths and Baraffe et al. (2002) evolutionary models strongly suggest that this association is $\ll$30 Myr. Observational evidence showing that some stars exhibit primordial levels of lithium, giant-like features in low-resolution spectra and the presence of infra-red excesses indicate that the association is considerably younger than 30 Myr and is a potentially valuable target for age determination using the Lithium Depletion Boundary method.

Subject headings: open clusters, lithium, Collinder 70

1. Introduction

Initial observations indicated a group of 55 A and B stars around Epsilon Ori (or Alnilam), a B0 super giant located in the Orion constellation. According to the initial mass function, this collection of high-mass stars would indicate hundreds of low mass stars in the vicinity, but these stars had yet to be studied. This grouping of high- and low-mass stars is called open cluster Collinder 70, otherwise known as Epsilon Ori. Collinder 70 is amenable to in-depth analysis since it is close (roughly 400 pc away), and located out of the galactic plane and away from the galactic center, thus reducing extinction and contamination of foreground and background stars. B0 stars like Alnilam are estimated to live about 10 Myr, and as a member of Collinder 70 indicates youth that would provide a unique snapshot of stellar evolution. If Collinder 70 is less than 10 Myr old, we would hope to find low-mass stars moving onto the main sequence, higher mass stars beginning to

[1]Macalester College, Research Assistant for CTIO 2012 REU program

[2]Visiting Astronomer, Cerro Tololo Inter-American Observatory (CTIO). CTIO is operated by AURA, Inc. under contract to the National Science Foundation.

[3]Fullbright Scholar, CTIO

[4]Post-Doctorate Research Scientist, Dept of Physics & Astronomy, Vanderbilt University

[4]Post-Doctorate Research Scientist, Dept of Astronomy, University of Michigan - Ann Arbor

burn helium in their cores, Classical T Tauri stars with thick circumstellar disks emitting infrared excess, and giant-like pre-main sequence (PMS) stars.

Open clusters in general are of particular interest because they are an excellent test bed for stellar evolution astrophysics. Since the stars formed from the same molecular cloud, they should have the same age, metallicity, distance, proper motion and systemic velocity. These parameters therefore provide a homogeneity to allow comparison between stars within the cluster.

While none of these parameters are easy to quote with certainty, the age of a cluster can act as a timestamp for the observed stellar processes. As a cluster ages, more solar-type stars contract, expel circumstellar disks and interstellar dust, and join the main sequence. More massive stars will burn through the hydrogen fueling fusion and evolve into red giants or traumatically explode into supernovae. Models exist to describe a star of a certain mass, metallicity, and temperature at a particular age, but it is difficult to verify these models without a precise age. Yet, how does one age a cluster of stars? The three methods used to analyze Collinder 70 were isochronal fitting to the upper and lower main sequence —"turn-on" and "turn-off" ages — and calculating the amount of lithium in the stars, known as the lithium depletion boundary age. The isochrone fitting methods are degenerate to distance, metallicity, and age. In an attempt find another age not completely dependent on photometry, this paper will focus on the spectroscopically identified lithium depletion boundary age to compare to the other two methods in the future. Lithium abundances are currently derived for seven clusters, hence independently listing three ages for the same cluster is a unique check on accepted stellar models.

1.1. Lithium Depletion in Stars

Before diving into the research, I would like to introduce the theory behind measuring the amount of lithium in Collinder 70. The lithium depletion boundary, sensitive to temperature, mass and age, is a consequence of the ephemeral nature of lithium. Essentially, lithium is easy to destroy yet difficult to create. Lithium burns in stars once the core reaches the threshold temperature of 3×10^6 K (Jeffries & Naylor 2001). It is depleted more rapidly in low mass stars since the convective cores reach deeper in the star and continuously renew the material in contact with the threshold temperature (Jeffries & Naylor 2001). If a star has lithium abundances at the primordial amount, this would hint towards a star that has not reached this temperature in its core.

Measuring the lithium absorption feature can be difficult since it is sensitive to many conditions. For example, young stars commonly rotate rapidly, producing broad lines which cannot be robustly modeled by a Gaussian function, and may include other nearby absorption features. Pre-main sequence (PMS) stars with a thick circumstellar disk may be veiled, which result in hot continuum emission filling in an absorption line. Veiling, originally described in (Calvet & Gullbring 1998) and common in Classical T Tauri stars, is from a shock forming in the photosphere caused by accreting matter in the circumstellar region.

2. Data Collection

Data was collected at Cerro Tololo Inter-American Observatory (CTIO) using two different telescopes on the summit over the course of a week.

2.1. Spectroscopy

Low resolution spectroscopy was taken with the HYDRA fiber multi-object spectrograph at the Cassegrain focus of the CTIO 4-meter Blanco telescope during the nights of 12 and 13 January 2012. The blue-blocking filter GG385 was used in conjunction with the first order grating of KPGL2 reflection spectrograph. 2 pixel resolution of R = 1300 covered the wavelength range from 3700 - 7500 Å, centered at roughly 6000Å, resulting in a 42.34 Å per 2 pixel dispersion. A HeNeAr lamp was used for calibration of the fibers.

HYDRA was again used for the high resolution data acquisition on 16 January 2012, but with the eighth order of the KPGL2 grating rather than first order. Combined with the E6757 filter and three 20 minute exposures, a resolution of R 21500 for 2 pixels and a dispersion of 0.308 Åper 2 pixel was achieved. The high resolution spanned from 6490 - 6760 Åcentered around 6650Å, and a ThAr lamp was used since it has distinguishable features in this wavelength range. We reduced all spectroscopic data within the IRAF[1] environment in standard way. We took steps similar to those described in Section 2 (Data Observations and Reductions) of Cummings et al. (2012) to reduce the data from HYDRA for subsequent analysis described below.

2.2. Photometry

Photometric data for Collinder 70 was collected during 12 - 20 January 2012 on the CTIO 1-meter telescope with the Y4K Cam. The CCD is 4096 x 4096 50-micron pixels. Images were taken with B, V, R, and I filters with typical integration times of 10, 8, 7, and 5 seconds, respectively. Photometry in the Johnson-Kron-Cousins photometric system (BV or UBV) was taken for standard stars. Aperture photometry was done on all of the pointings (Figure 1). A few stars were later identified to have close neighbors, therefore point spread function fitting was undertaken in order to isolate the target stars.

3. Target Selection

Target selection began by using the photometric data to create a color magnitude diagram (CMD) of V v. $(V - I)_c$. The CMD (Figure 2) includes Collinder 70 field stars (black dots) with red circles around stars later identified with measurable lithium abundances, as described in 4.1. These

[1]IRAF is distributed by the National Optical Astronomy Observatory, which is operated by the Association of Universities for Research in Astronomy, Inc. under contract to the National Science Foundation.

red encircled stars populate near the 10 Myr isochrone from D'Antona & Mazzetelli (1997), highlighting the fact that target selection began with picking stars around this model isochrone. The isochrone is degenerate with respects to age, distance, metallicity, and reddening, thus changing these parameters alters which stars cluster around the model isochrone. In other words, if I were to slightly change the metallicity or distance of the model isochrone, I could manipulate the other parameters such that the isochrone would appear in the exact same location as shown in (Figure 2), yet would represent a completely different set of stars. These two isochrones would appear to be identical only illuminating the shortcomings of the isochronal models.

These 70 stars then underwent low resolution spectroscopic observations spanning nearly 4000 Ås of wavelength space for initial detection of lithium as described below in Section 4. The low resolution also allows us to rule out background giants by discounting stars with redshifted high mass spectral types. For example, Figure 3 is one low resolution spectra that has Hα emission, Li absorption for a low-mass star spectral type — thus a Collinder 70 candidate.

Next, high resolution (Figure 4) spectroscopy was collected in order to measure the neutral lithium, Hα and radial velocity of each target star. How these measurements are made is described below in Section 4. Any star with neutral lithium are considered members until further observations can conclusively discount them.

4. Measurements

4.1. Lithium I equivalent widths (Li I EW)

To measure the amount of lithium, we used two different methods to derive the equivalent width of a normalized spectra — direct integration and Gaussian fitting. Direct integration is sensitive to noise in the absorption line while Gaussian fitted methods can more easily measure an equivalent width regardless of spikes, as shown in Figure 5. For error of the lithium measurements, we used the Jeffries et al. (2009) equation

$$\sigma\mathrm{EW} = \left[1.5\sqrt{(\mathrm{pw})}\right]/\mathrm{SNR} \tag{1}$$

In this equation, p is pixel size, w is the full width half max of the absorption feature, and SNR is the signal to noise ratio for each spectrum. We measured SNR around a pseudo continuum 10 piece of the spectrum centered at 6600Å. If a star had no lithium absorption line, we used the full width half max (FWHM) of the Fe I (6677Å) or Ca I (6718Å) line to estimate a 3σ upper limit for lithium in the star.

To check if these two methods for measuring absorption features are robust, we plotted direct integration EW vs Gaussian fitted EW for all stars with Li, as shown in Figure 6. Member stars jump out above 200 mÅ with most of the stars falling along the equivalency line. The apparently errant stars appear spectroscopically as broad features, possibly indicating stars that are rapidly rotating but still contain lithium.

4.2. Hα equivalent widths (Hα EW)

Gaussian fitting was used to measure Hα, and a note was made whether the feature was in absorption or emission. This measurement was mostly made because Hα in emission is correlated with finding Li I. Also, a star with Hα EW >10Å is probably a classical T Tauri (CTT) star with a thick circumstellar disk and infrared excess. As defined in Bertout & Bouvier (1989), a CTT is distinguished from Weak Line T Tauri (WTT) star by the strength of the Hα emission line. If the line strength is greater than 10Å, it is usually classified as a CTT. For example, probable Collinder 70 member F-41 with Li EW of 357±16 mÅ has Hα emission that dwarfs any other feature with an EW of 51Å (Figure 7).

4.3. Radial Velocities

The high resolution spectra was used to find the radial velocities of the stars by cross correlating the target spectra with a radial velocity standard star using IRAF's FXCOR. After acquiring the radial velocities, the data was processed to ascertain whether the velocities suggest the presence of a cluster of co-moving stars. Using three different bin sizes of 2, 3, and 4 km/s and shifting the centers by 0.5 km/s, histograms were produced with all the stars – those with and without Li I – with radial velocities. A Gaussian function is fit to the radial velocities of the Li rich stars, which are indicated by the hatched regions of the histogram, in order to check how the center and sigma values vary depending on the binning of the data. Fortunately, these twelve tests give a Gaussian center of 30 km/s ± 0.5 km/s. From these histograms we can garner that the radial velocities suggest a group of lithium rich stars moving at a systemic velocity of 30 km/s.

The stars likely to be in Collinder 70 do not create a delta function (i.e., all the stars do not have the same radial velocity) for a variety of reasons. First, there may be contaminating stars with lithium that happen to be in the field, or an errant absorption line could have been measured as lithium. A lithium rich star in a short-term, close binary will be drastically shifted away from the systemic velocity. With repeated observations of these stars, the binaries will be apparent. Stars within a cluster have some natural intrinsic velocity since they are not completely still in relation to each other. Lastly, these histograms are comprised of a few dozen stars and the Gaussian functions are fit to roughly 30 stars. With more stars in hand, we would expect to find more stars populating the 30 km/s velocity bin.

4.4. Reddening of Stars in the Cluster

Finding the reddening of the cluster proved to be a great challenge. The hot stars such as Alnilam indicate a reddening of 0.4 by using stellar classification to compare standard stars and target stars. Unfortunately, this type of analysis for the target stars is difficult because the spectra are skewed since many appear to be PMS or have circumstellar disks. In addition, circumstellar disks and remnant gas in the cluster introduce differential reddening, reducing the chances of finding one "true" blanket reddening value.

For this paper, reddening is found by using Ramirez & Mendelez (2005) temperature and photometric color relationships. We relate these temperatures to reddening. With a given reddening value, we have five different colors ($B-V$, $V-I$, $V-J$, $V-H$, $V-K$) for each star, and these five colors relate to a specific effective temperature. Taking the mean of these five temperatures provides a standard deviation for a reddening value. We repeated this process for every star with reddening values from 0.1 to 1 in increments of 0.1, giving 99 STDEV for each star. At some point, the STDEV is minimized giving us a specific reddening value for that star; see Figure 8 for an example plot. If a star's reddening value is at a minimum at 0.1, we applied the standard hot star reddening value of 0.4. This is a novel way to find reddening, and has not yet been proven to be valid. There are not many ways to find the reddening, and the conventional way using stellar types was not a viable option due to the lack of standard low mass stellar spectra in the literature. In the future we hope to compare this method to others, or find another way to find the reddening.

5. Discussion

To begin, we were curious where Collinder 70 stars fall along evolutionary tracks in a color-color diagram such as Figure 9. This figure includes field, Collinder 70 Li-rich, and Orion Classical T Tauri (CTT) stars. Fortunately, we see stars that appear giant-like — or stars that have not moved onto the main sequence and are therefore still contracting. A few stars have infrared excess, located near other CTT stars since they are circumstellar disks that re-radiate light in the infrared. Finally, a handful of stars are on the main sequence. These lithium abundant stars in the giant-like and IR excess regions are great indicators of stellar youth.

With the lithium equivalent widths, 3σ upper limits, and individual reddening corrected colors in hand, Figure 10 is produced to age a cluster using the Lithium Depletion Boundary method. This figure is based on Jeffries et al. (2009) Figure 6, utilizing model isochrones for lithium depletion from Baraffe et al. (2002) evolutionary models to age target stars on an EW and color diagram. Stars cannot easily shift up or down since this is reliant on the amount of lithium, but can move significantly left and right depending on the reddening value. As mentioned in Sect 4.4, each star has a unique reddening value, but this value may not be correct. By changing this value, a star's nearest isochrone can drastically change as the star shifts location.

Looking at Figure 10, Collinder 70 stars (encircled in red) appear to fall anywhere from above the undepleted lithium level to below the 100 Myr isochrone. From this graph, any conclusions regarding Collinder 70 age would be dependent on small number statistics from 23 member stars, and thus not statistically robust. With further observations of low mass stars, there will naturally be more data points to populate this graph and better constrain the age of the cluster using the Lithium Depletion Boundary method.

6. Conclusion

The observation of stars in Figure 10 at the undepleted level is yet another piece of evidence that points to a young cluster. This piece of data, along with other indicators of youth present in

Collinder 70, such as giant-like PMS stars, Classicial T Tauri stars and large, hot B0 stars like Alnilam, suggest that Collinder 70 is younger than 10 Myr. Future observations of Collinder 70 will increase the number of detected target low-mass stars, adding more points to Figure 10. The location of the stars in this figure will illuminate the strengths and weaknesses of the Lithium Depletion Boundary models as compared to photometric isochronal fitting models. Although the LDB method is not foolproof, it provides the possibility of spectroscopically aging a cluster, complementing early and late type stellar isochronal fitting. In the end, each method of aging stars allows researchers to calibrate and constrain stellar evolution models that further our understanding of how stars change with time.

7. Acknowledgments

I would like to acknowledge Dr. David James for acting as my research mentor during the CTIO REU program, and Owen Boberg for teaching me basic Python. Thank you to Catherine Kaleida and the staff at CTIO for your assistance and creating a welcoming environment in Chile. This project was conducted in the framework of the CTIO REU Program, which is supported by the National Science Foundation under grant AST-1062976, and was additionally supported by the NSF Astronomy & Astrophysics Grant AST-1109612 (P.I. Cargile).

REFERENCES

Baraffe, I., Chabrier G., Allard F., Hauschildt P.H. 2002, A&A, 314, 173

Bertout, C. & Bouvier, J., 1989, in B. Reipurth (ed.), Low Mass Star Formation and Pre-Main Sequence Objects, ESO Workshop, p. 215

Bodenheimer, P. 1965, ApJ, 77, 455

Calvet, N. & Gullbring, E., 1998, ApJ, 509, 802

Cummings, J.D., Deliyannis, C.P., Anthony-Twarog, C., Twarog, B. & Maderak, R.M., 2012, AJ, 144, 137

D'Antona, F. & Mazzetelli, I., 1997, Mem. S. A. It., 68, 807

Jeffries, R.D., Jackson, R.J., James, D.J., Cargile, P.A. 2009, MNRAS, 400, 317

Jeffries, R.D. & Naylor, T. 2000, in Astronomical Society of the Pacic Conference Series, Vol. 243, From Darkness to Light: Origin and Evolution of Young Stellar Clusters, ed. T. Montmerle & P. André, 633

Lejeune, T. & Schaerer, D., 2001, A&A, 366, 538

Ramirez, I. & Mendelez, J., 2005, ApJ, 626, 446

This preprint was prepared with the AAS LaTeX macros v5.2.

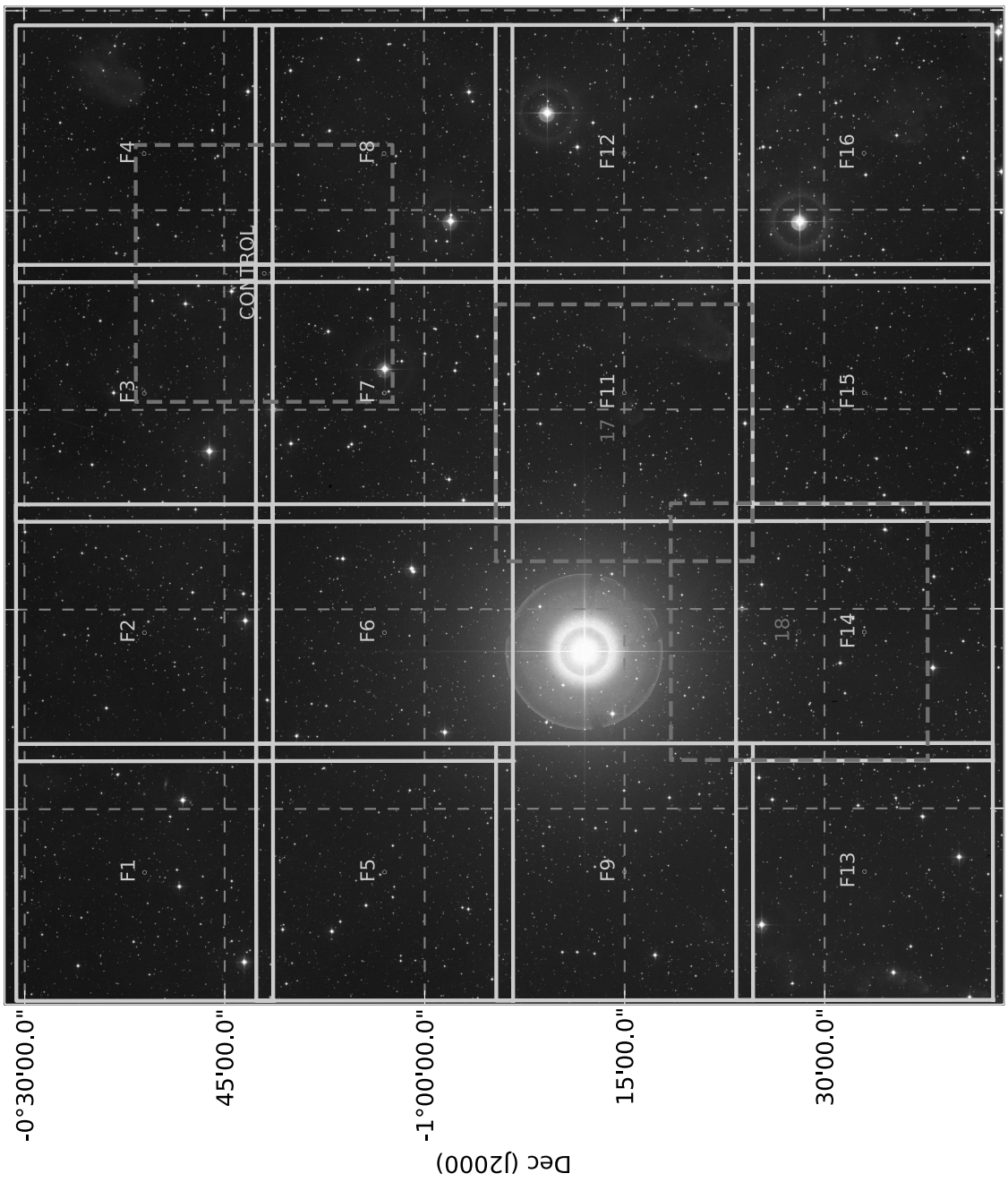

Fig. 1.— Pointings for Collinder 70 for photometric data collection are outlined in green and red. The bright center star is ϵ Ori, or Alnilam.

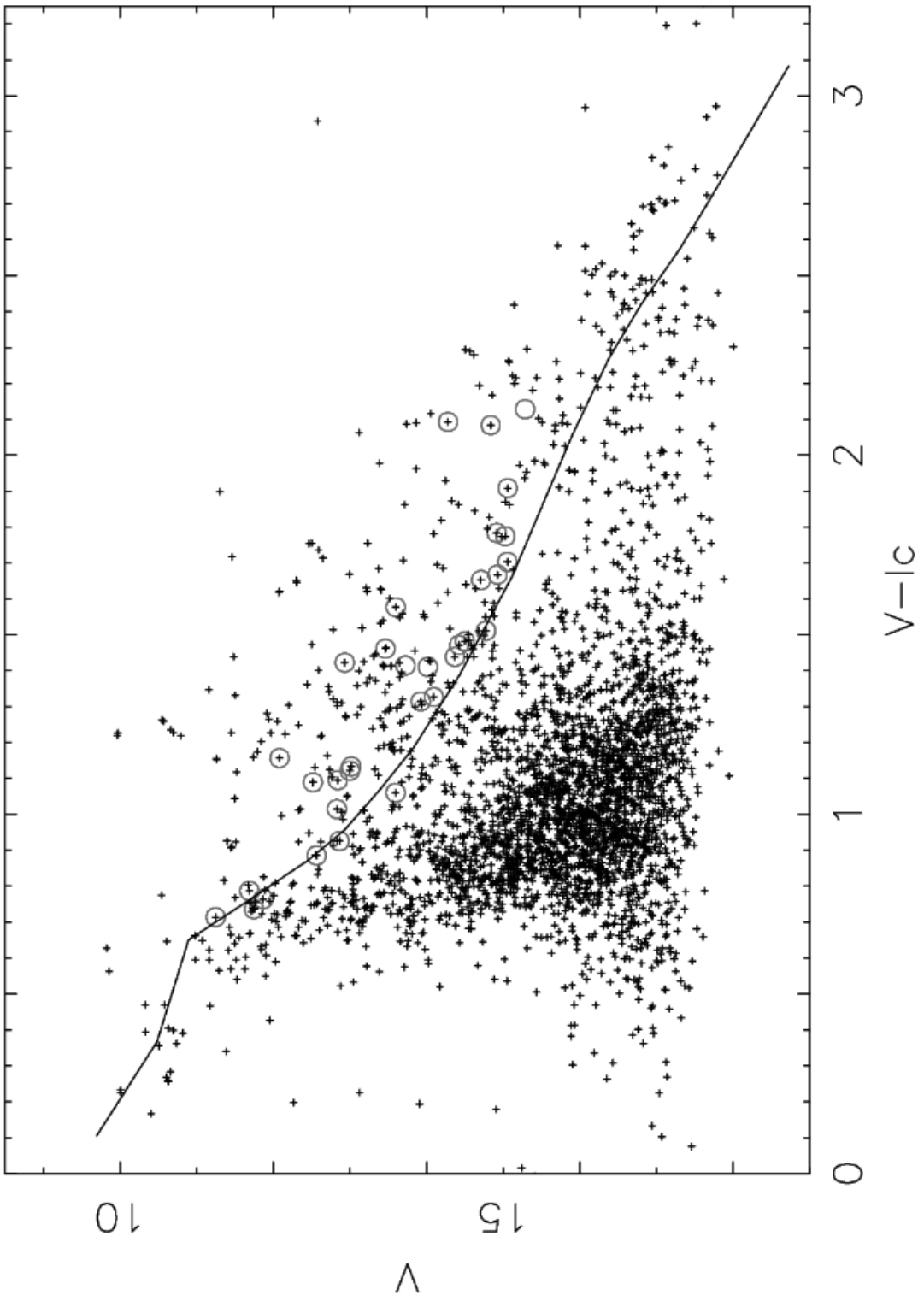

Fig. 2.— Color-magnitude diagram of Collinder 70, focusing on the low mass stars. Stars later identified as Li rich are encircled in red.

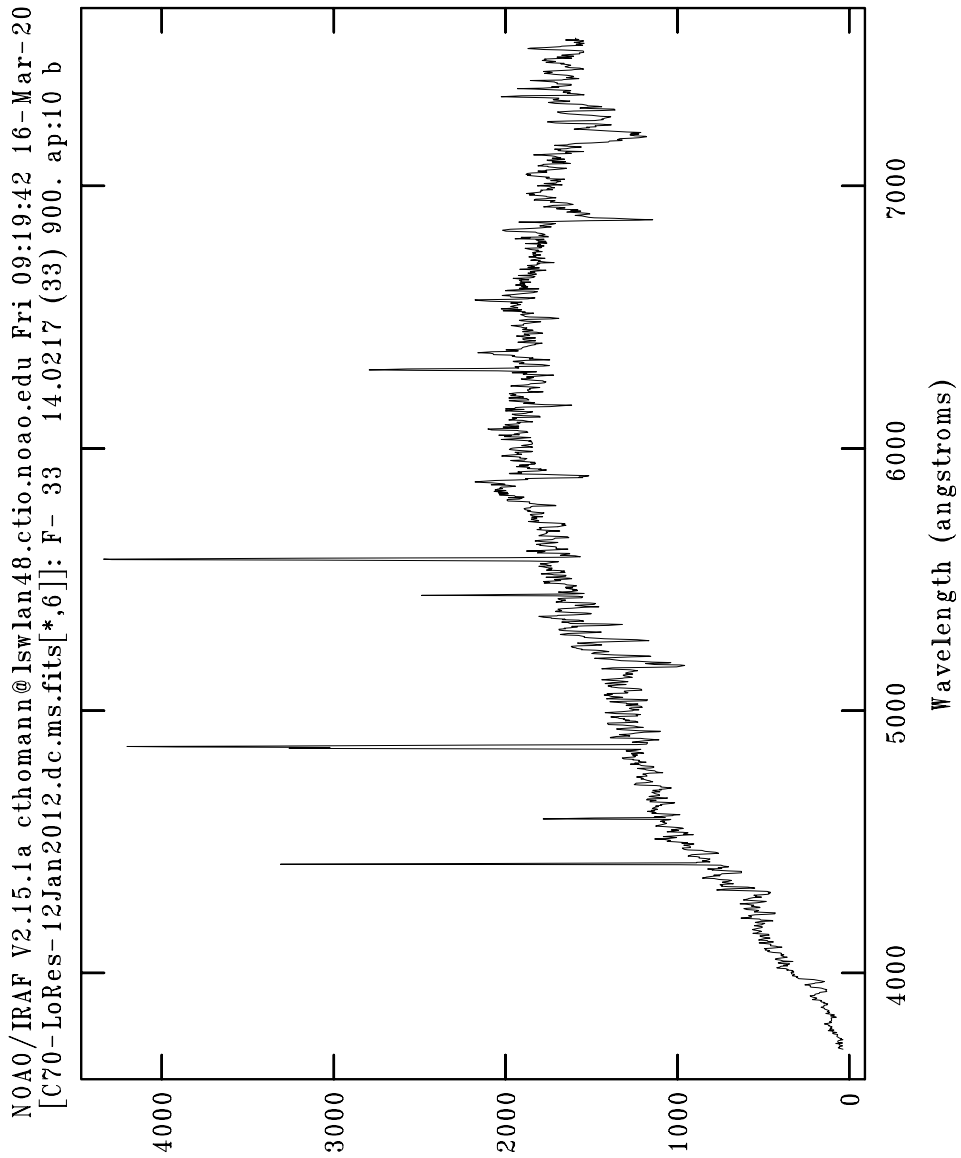

Fig. 3.— Low resolution spectrum of Collinder 70 member F-33. This spectrum is used for identifying Hα (6562.8 Å) emission and Li I (6707.8 Å) absorption and spectral classification.

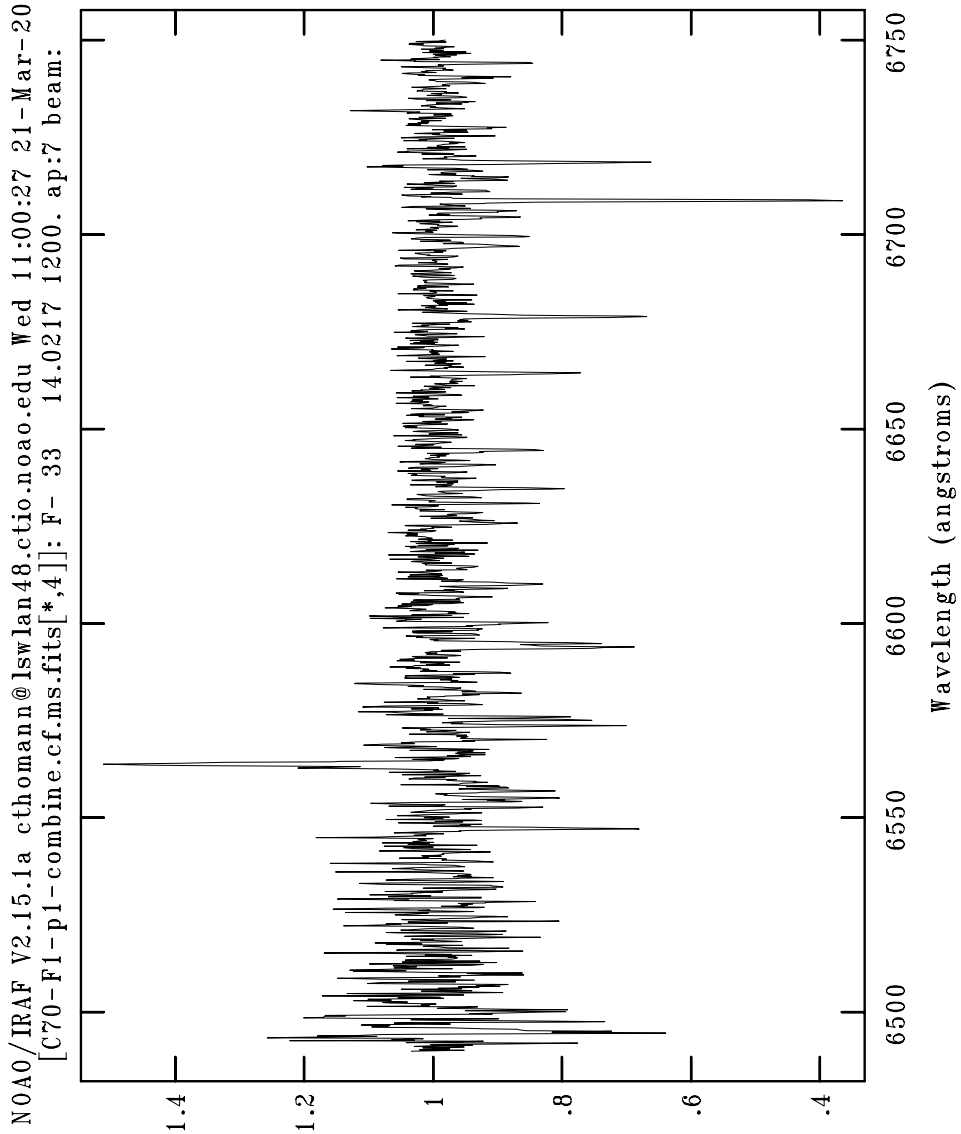

Fig. 4.— High resolution spectrum of Collinder 70 member F-33, a late K or early M class star. Hα (6562.8 Å) emission and Li I (6707.8 Å) absorption are clearly visible, indicating a possible member of Collinder 70. Note the wavelength range is significantly smaller than Figure 3.

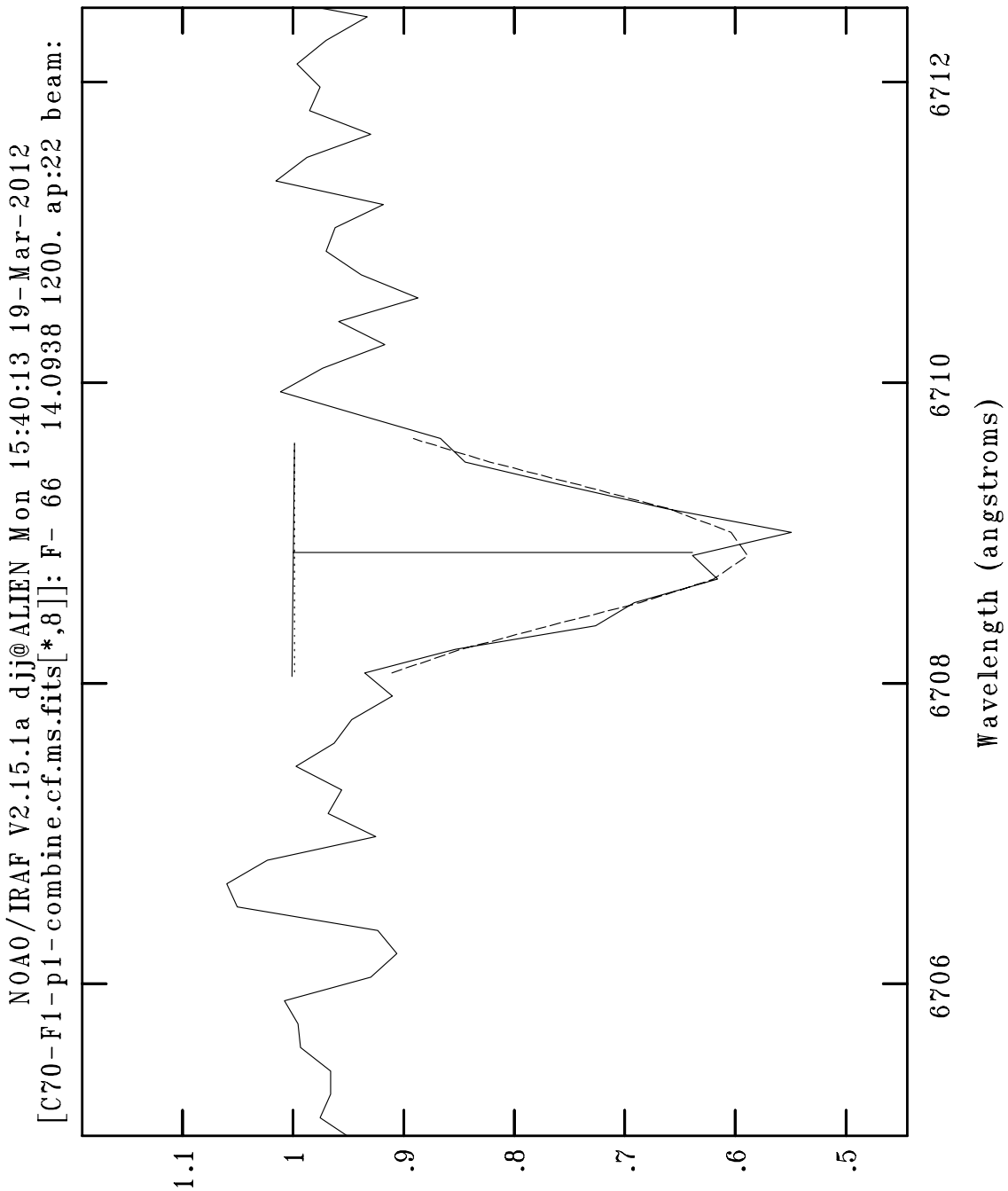

Fig. 5.— Example of the two methods to measure Li EW — Gaussian fitting is the dotted line, direct integration is the solid "T"-shaped line.

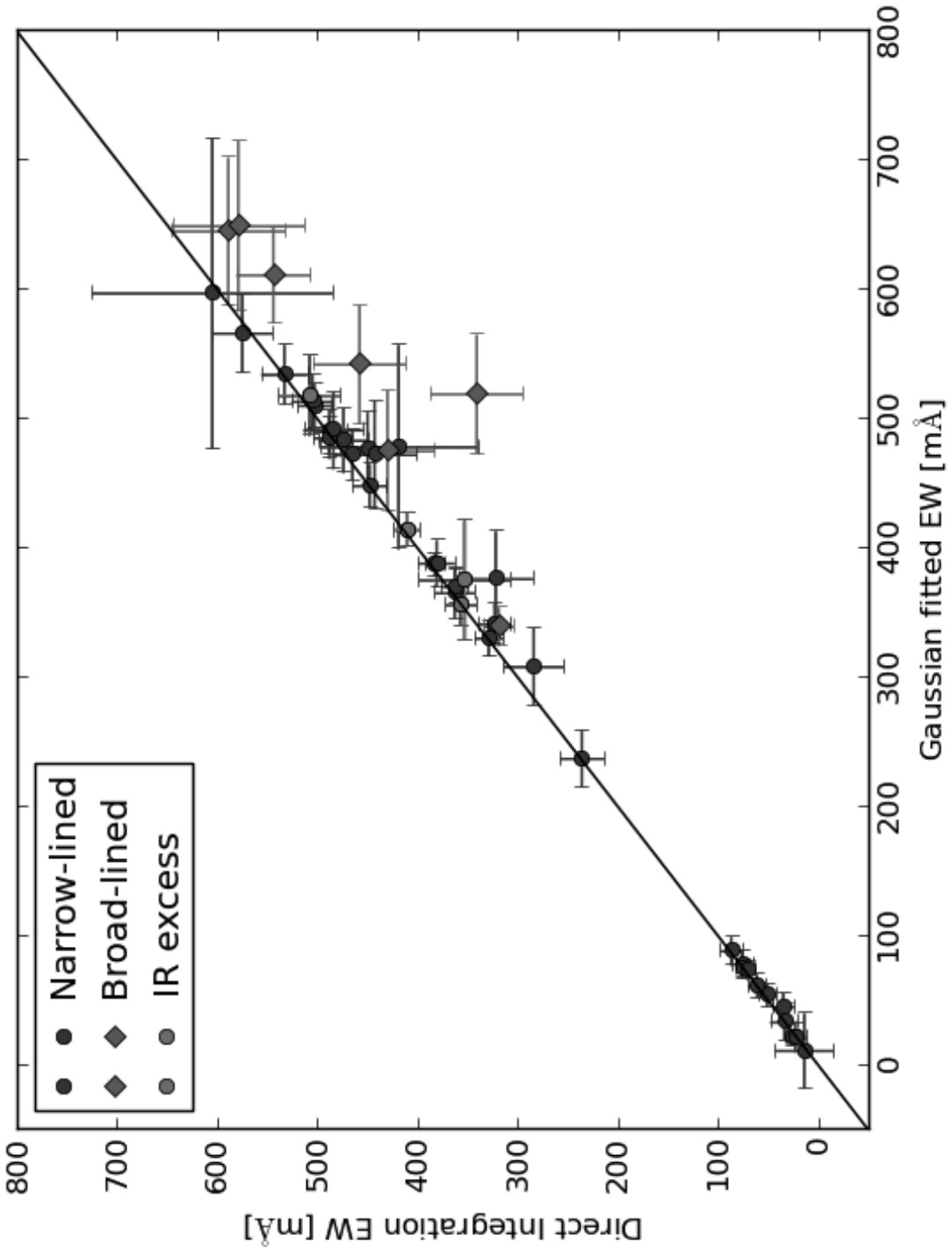

Fig. 6.— Plot demonstrating the accuracy between the Gaussian fitting and direct integration. Note that the only stars not falling along the equivalency line are broad-lined features of Li I absorption.

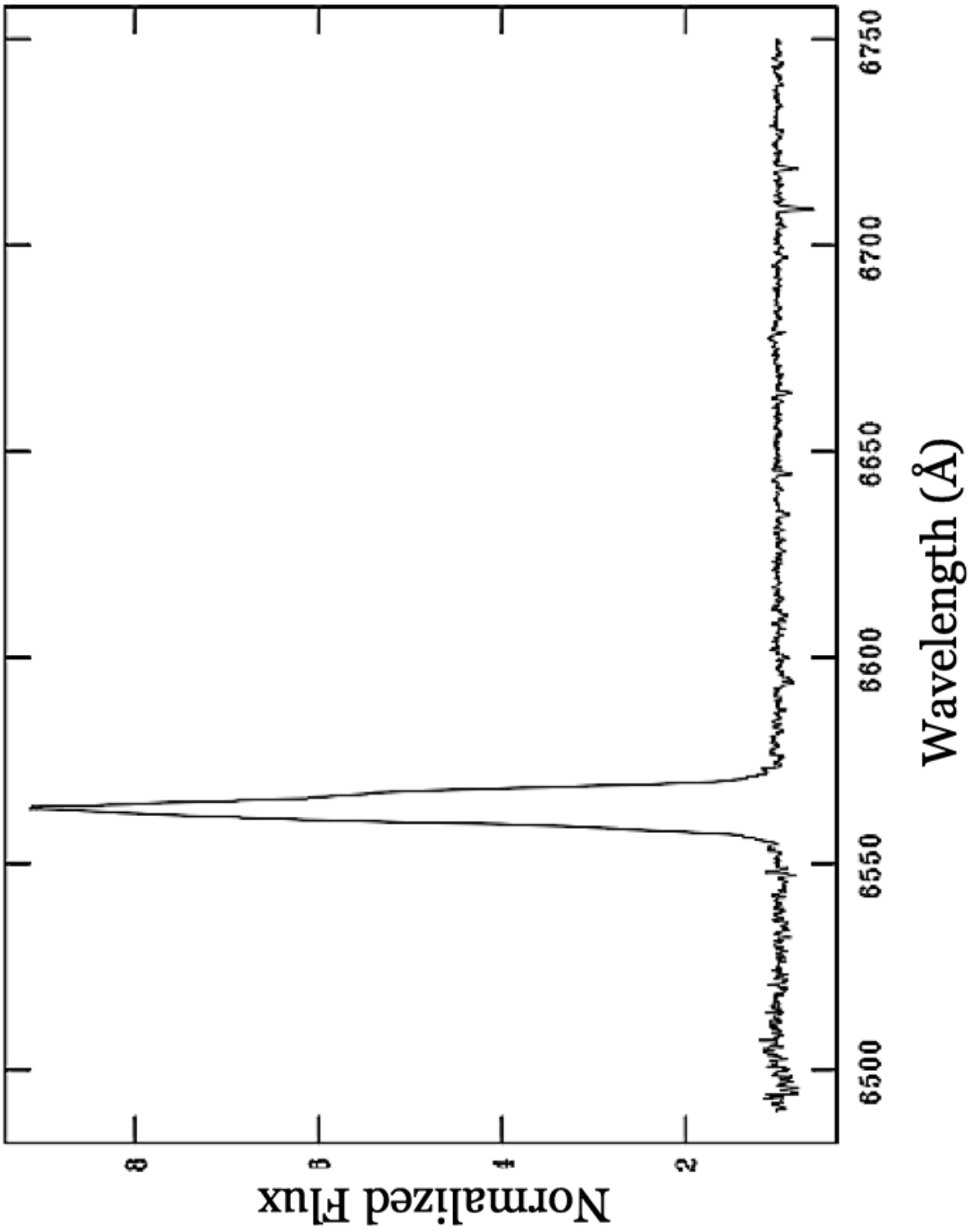

Fig. 7.— Example of Hα excess indicating a possible CTT: probable Collinder 70 member F-41 with Li EW of 357±16 mÅ has Hα emission (EW = 51Å) that dwarfs any other feature.

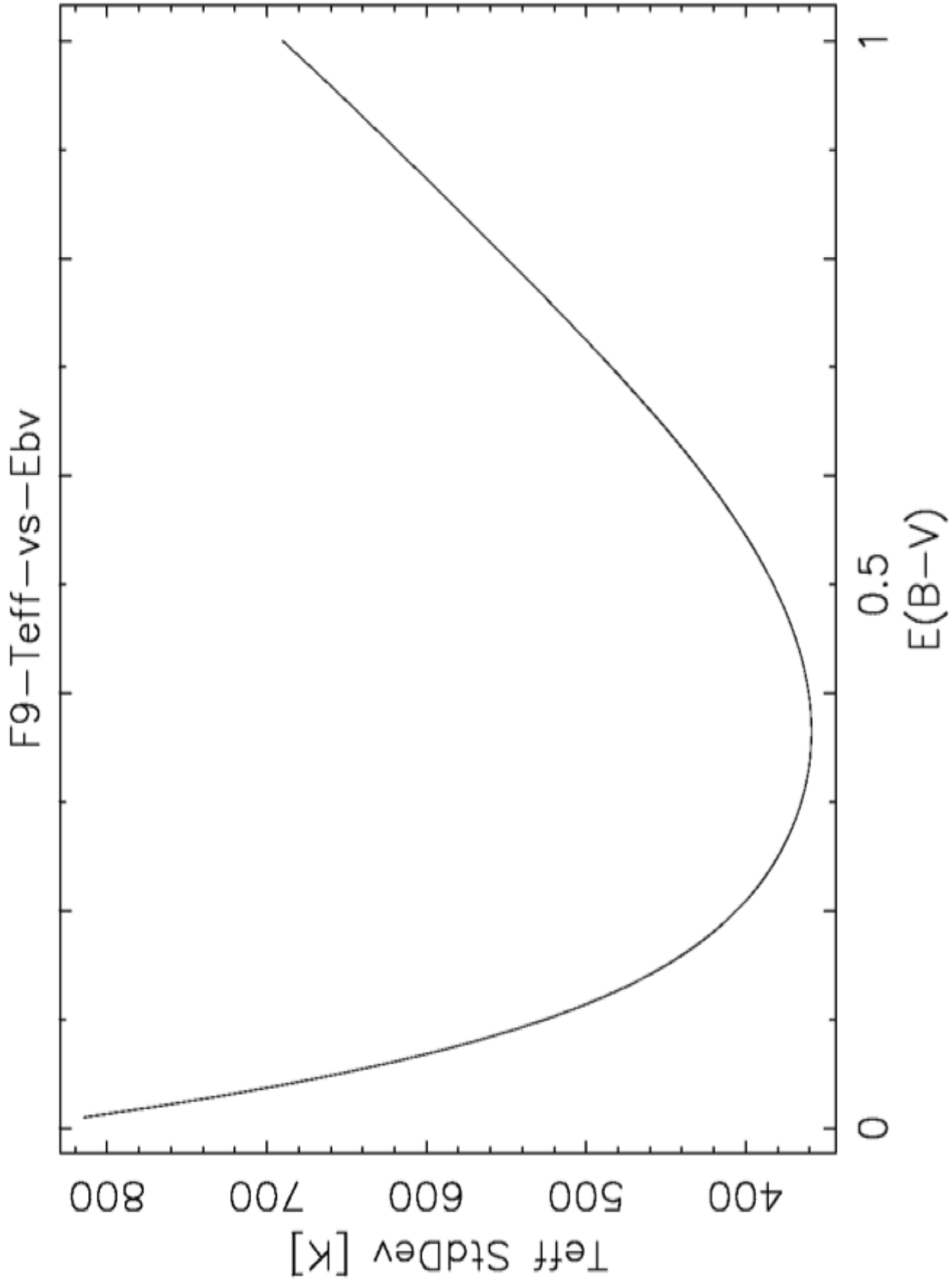

Fig. 8.— Method to find the reddening value for an individual star. This particular star – F-09 – has a reddening value of 0.37.

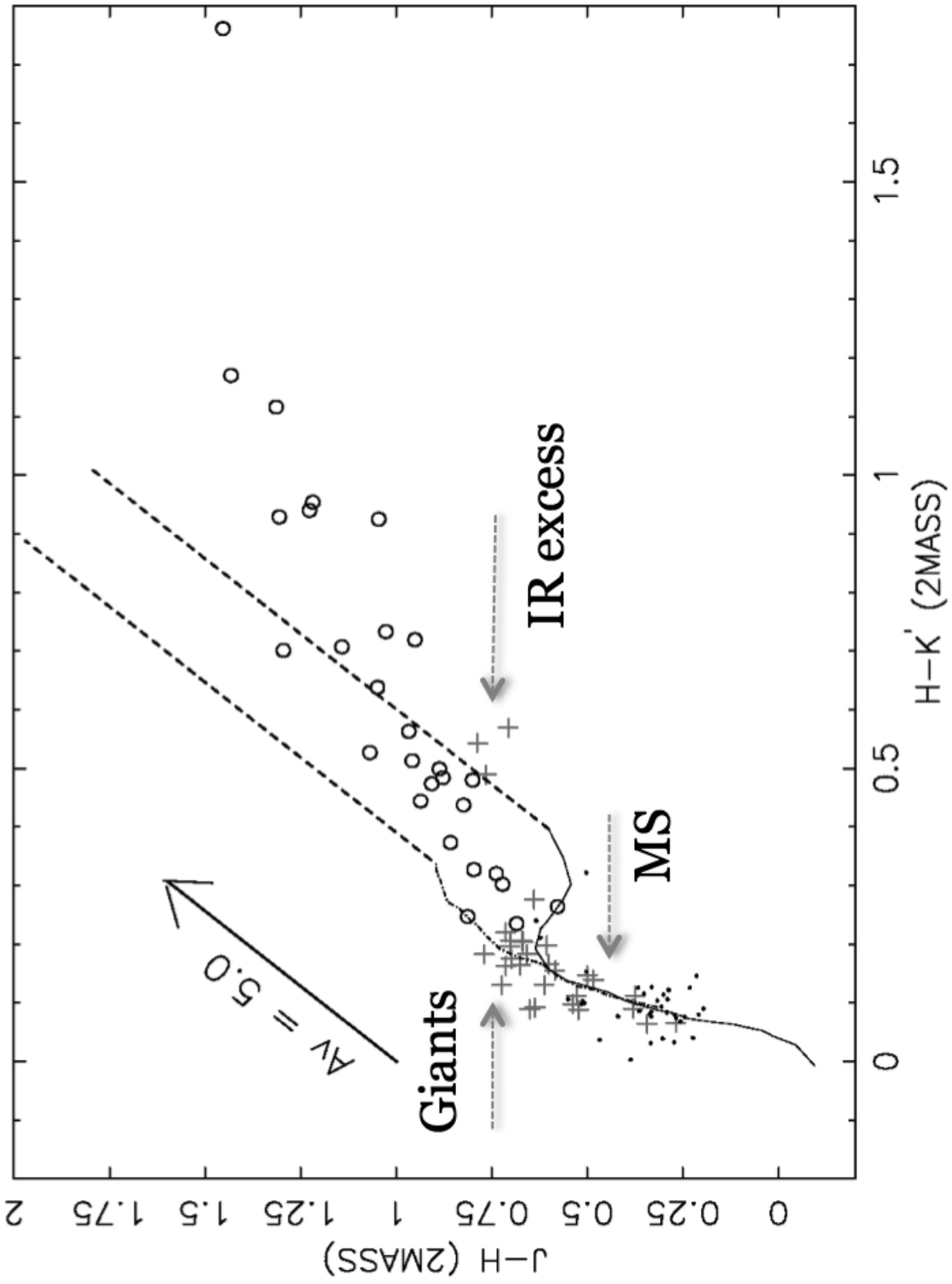

Fig. 9.— Color-color diagram with field stars (black dots), Orion classical T-Tauri stars (black open circles) and Collinder 70 stars (red crosses). This diagram demonstrates that some member stars appear giant-like while others have infrared excess — both properties are indicators of young stars.

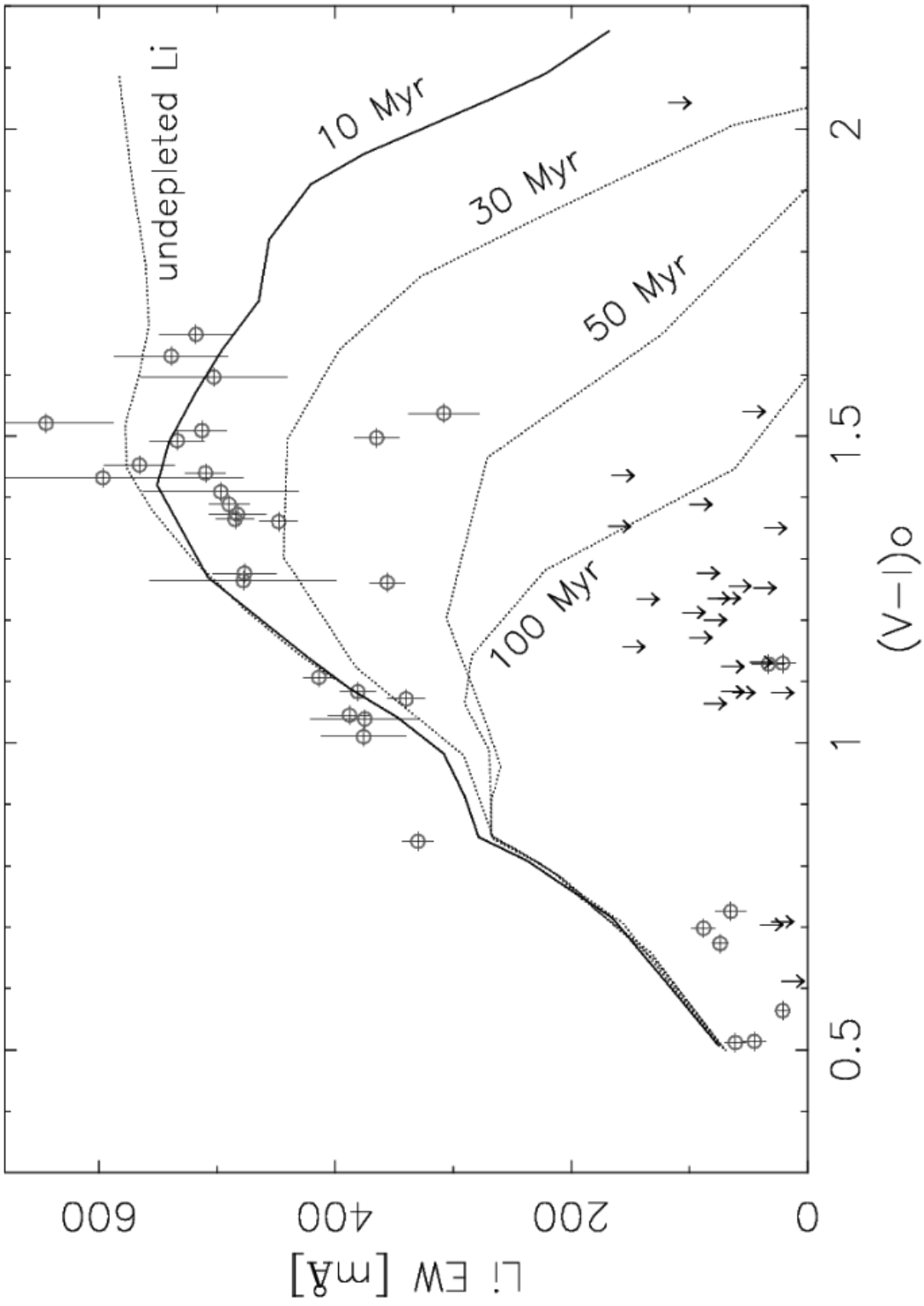

Fig. 10.— Model isochrones from Baraffe et al. (2002) evolutionary models overlaid on Collinder 70 Li-rich stars with respective errors; arrows represent 3σ upper limit. Some stars are above the undepleted Li level, while others are older than 30 Myr.

Table 1: Spectroscopic, Li EW, Hα EW, and error results for Collinder 70 member stars

Star	Ap	RA (2MASS) J2000	Dec (2MASS) J2000	Li EW Integration (mÅ)	Li EW Gaussian (mÅ)	w (Å)	SNR	Ha	σ (mÅ)	Comments
F-20	8	05 33 22.77	-01 12 33.67	–	–	0.4802	23	–	18	FWHM - Ca I, Ha = absorp
F-21	84	05 33 23.24	-01 23 07.26	–	–	0.5045	32	–	13	FWHM - Ca I, Ha = absorp
F-24	20	05 33 26.69	-01 17 12.59	76	78	0.6102	42	–	11	absorp, possible core
F-25	50	05 33 27.91	-01 09 25.70	–	–	0.5120	40	–	11	FWHM - Ca I, Ha = absorp
F-28	49	05 33 29.93	-01 11 16.40	503	510	0.8703	32	2.10	17	overt emission
F-31	1	05 33 31.46	-01 00 17.24	505	513	0.7552	24	1.42	21	overt emission
F-39	131	05 33 42.08	-01 25 13.66	319	339	1.3960	45	0	15	filled-in, emission core?
F-41	141	05 33 43.26	-01 08 34.68	357	356	0.8098	34	51	16	massive emission
F-42	58	05 33 43.73	-01 23 42.28	71	73	0.6341	69	–	7	Ha = absorp
F-43	81	05 33 43.91	-01 20 37.02	–	–	0.5367	29	–	15	FWHM - Ca I, Ha = absorp
F-46	105	05 33 47.02	-00 56 38.13	–	–	0.5216	16	–	27	FWHM - Ca I, Ha = absorp
F-48	55	05 33 49.19	-01 15 45.53	465	472	0.6805	24	0.68	20	overt emission
F-52	28	05 33 52.06	-01 04 25.50	–	–	0.8378	34	–	16	FWHM - Ca I, Ha = absorp
F-53	145	05 33 57.54	-00 52 45.51	363	365	0.7209	25	1.39	20	overt emission
F-54	47	05 34 01.48	-01 14 35.60	–	–	0.5349	44	–	10	FWHM - Ca I, Ha = absorp
F-58	10	05 34 06.41	-01 01 48.92	575	566	0.7693	17	2.11	30	overt emission
F-61	119	05 34 08.58	-01 22 46.80	579	649	2.4520	14	4.31	66	overt emission
F-63	88	05 34 11.34	-01 30 31.49	430	475	3.1240	22	1.33	47	overt emission
F-65	26	05 34 12.83	-01 20 37.91	383	387	0.6499	53	0.5	9	emission core
F-71	100	05 34 24.34	-00 55 56.99	35	45	1.0720	57	–	11	Ha = absorp
F-72	124	05 34 27.46	-00 57 15.31	–	–	0.5294	14	–	31	FWHM - Ca I, Ha = absorp
F-75	35	05 34 34.69	-00 51 34.00	419	478	0.8935	7	1.21	79	overt emission
F-76	93	05 34 36.22	-01 01 02.08	–	–	0.4234	37	–	10	FWHM - Ca I, Ha = absorp
F-77	82	05 34 39.64	-00 58 14.20	–	–	0.5293	16	–	27	FWHM - Ca I, Ha = absorp
F-78	139	05 34 40.97	-01 22 44.21	443	472	1.1380	15	3.22	42	overt emission
F-79	9	05 34 41.08	-01 12 05.45	–	–	0.5831	21	–	21	FWHM - Ca I, Ha = absorp
F-87	91	05 34 49.74	-01 06 27.25	61	61	0.5910	51	–	9	Ha = absorp
F-88	25	05 34 54.92	-00 57 30.84	411	414	0.7036	37	7.73	13	overt emission
F-90	32	05 34 56.92	-01 22 54.72	544	611	1.4440	19	3.22	37	overt emission
F-93	27	05 34 58.20	-01 12 37.90	381	388	0.7559	28	0	18	fill-in
F-94	41	05 34 58.26	-01 10 20.38	–	–	0.5265	8	–	53	FWHM - Ca I, Ha = absorp
F-98	18	05 35 09.10	-01 20 06.06	322	376	1.2650	18	0.32	37	overt emission
F-101	104	05 35 12.77	-00 54 52.79	–	–	0.6414	9	–	52	FWHM - Ca I, Ha = sky only
F-102	108	05 35 13.13	-01 06 24.93	–	–	0.5671	9	–	49	FWHM - Ca I, Ha = absorp
F-104	112	05 35 15.73	-00 59 11.90	474	483	0.7910	21	1.47	25	overt emission
F-105	30	05 35 15.93	-01 20 46.36	–	–	0.7355	11	–	46	FWHM - Fe I, Ha = absorp
F-107	33	05 35 18.32	-01 16 19.99	–	–	0.5974	21	–	22	FWHM - Ca I, Ha = absorp
F-110	123	05 35 22.93	-01 11 24.27	353	375	0.8929	12	7.99	46	overt emission (disk?)
F-111	43	05 35 23.40	-00 55 36.85	–	–	0.4342	12	–	32	FWHM - Fe I , Ha = absorp
F-121	2	05 35 39.16	-01 11 49.08	605	597	1.0340	5	3.65	12	overt emission